A New Fast and Blind Cross-Polarization Modulation Digital Compensator

P. Serena[(1)], A. Ghazisaeidi[(2)], A. Bononi[(1)]

[(1)] Università degli Studi di Parma, dept. Ingegneria dell'Informazione, v.le G. P. Usberti 181/A, 43124 Parma (Italy), ✉ paolo.serena@unipr.it

[(2)] Alcatel-Lucent, Bell Labs, Centre de Villarceaux, 91620, Nozay, France.

Abstract *We propose a novel blind feed-forward compensator of cross-polarization modulation for PDM-QPSK signals. Simulations show an improvement of 1 dB in Q-factor in a 112Gbit/s 2000km SMF dispersion-managed link.*

Introduction

Inter-channel nonlinear distortions are one of the most limiting factors in nowadays optical systems. Such nonlinearities depend both on the power and the state of polarization (SOP) of the wavelength division multiplexed (WDM) channels. The dependence on SOP is of special concern in polarization division multiplexed (PDM) systems, where the induced distortion is known as cross-polarization modulation (XPolM) to distinguish it from scalar cross-phase modulation (XPM) that just depends on the channels' power.

Several techniques to mitigate XPolM exist, operating in the optical or in the electrical domain. In the optical domain it is worth mentioning the use of time interleaved return-to-zero (iRZ) pulses[1], dispersion uncompensated links, or passive devices inducing channel walk-off. A comparison among such techniques can be found in[2]. In the electrical domain attempts to compensate cross-nonlinearities using digital back-propagation have been shown[3], but the high complexity and the inability to work in a networking scenario makes this option unattractive. A simple, decision-aided nonlinear polarization crosstalk canceler (NPCC) based on a perturbative approximation of the nonlinear crosstalk was introduced in[4]. The NPCC was shown to be a practical solution to partially suppress XPolM.

In this paper we propose a new blind feed-forward XPolM compensator for PDM quadrature phase shift keying (PDM-QPSK) signals, which does not require a perturbative assumption for the XPolM effect, and we test its effectiveness by means of numerical simulations.

The Algorithm

Fig. 1 (left) shows where the new fast XPolM compensator fits within the standard blocks of the digital coherent receiver. The slow polarization recovery block, implemented e.g. by a constant-modulus algorithm (CMA), equalizes linear single-channel distortions like polarization mode dispersion (PMD) and recovers the average polarization reference of the PDM signal over a very long block of thousands of symbols. Then the proposed fast XPolM compensator recovers fast polarization deviations from the average.

The operation of the new fast compensator is best understood by reasoning in the Stokes domain as shown in Fig. 2. Here an ideal PDM-QPSK signal maps onto four points placed at $\pm S_2$ and $\pm S_3$ over the Poincaré sphere. Such ideal points are rotated and spread out in clouds in presence of XPolM, as sketched by the four balls. Optimally recovering the distortion introduced by XPolM in a minimum mean square error (MMSE) sense requires finding the best regression plane fitting the data points making up the balls, and then aligning the polarization demultiplexer axes to it. These are the operations performed by the blocks of the fast XPolM compensator shown in Fig. 1(right). Indicating with $\vec{s}_k = [s_{1k},\, s_{2k},\, s_{3k}]^T$ a generic data point, with $\vec{v}_n$ the normal to the regression plane at time n, and with $\langle \vec{v}_n,\, \vec{s}_k \rangle$ the scalar product between $\vec{v}_n$ and $\vec{s}_k$, the normal $\vec{v}_n$ is the vector minimizing the function:

$$f(\vec{v}) \triangleq \frac{\sum_{k=n-L}^{n+L} |\langle \vec{v},\, \vec{s}_k \rangle|^2}{|\langle \vec{v},\, \vec{v} \rangle|^2} = \frac{\vec{v}^T \mathbf{Q} \vec{v}}{\vec{v}^T \vec{v}} \qquad (1)$$

being $\mathbf{Q}$ a 3×3 covariance matrix with entries equal to the averaged moments of inertia of $\vec{s}_k$, i.e., with elements $Q_{ij} = \sum_{k=n-L}^{n+L} s_{ik} s_{jk}$, and $2L+1$ is the number of symbols over which the fast sliding-window covariance matrix averaging is performed. The size of this window follows similar rules as the Viterbi and Viterbi (V&V) phase estimation[5]: it should be short enough to track the

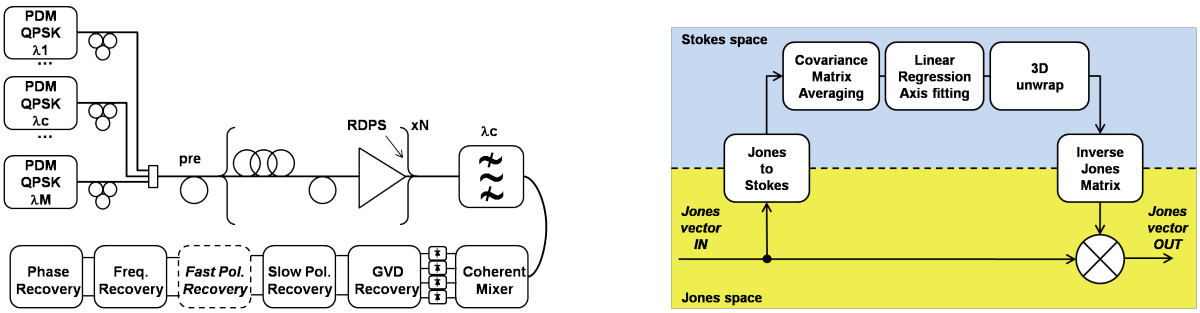

Fig. 1: Left: Optical link and DSP with the proposed XPolM compensator (Fast Pol. Recovery) in dashed line. Right: details of the Fast Polarization Recovery block.

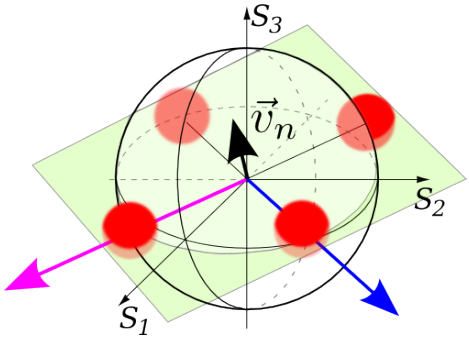

Fig. 2: Regression plane to the PDM-QPSK over the Poincaré sphere. Arrows: eigenvectors of matrix $\mathbf{Q}$; red balls: XPolM scattering. The equalizer rotates the plane bringing the black arrow over S_1.

fast polarization scattering, but also long enough to get a good noise averaging. In any case, it is always much shorter than the typical response time of the CMA block. The Rayleigh quotient $f(\vec{v})$ in (1) is minimized by the eigenvector of matrix $\mathbf{Q}$ associated with the smallest eigenvalue. Being $\mathbf{Q}$ a 3×3 matrix, such an eigenvector can be evaluated in closed form. Once the normal $\vec{v}_n$ has been identified (block "linear regression axis fitting" in Fig. 1), a 3D-unwrap function removes polarization cycle slips, and finally the rotation matrix that brings $\vec{v}_n$ onto the S_1 axis ("inverse Jones matrix" in Fig. 1) can be evaluated and applied. This way, the Stokes vectors $\vec{s}_k$ lie, in a MMSE sense, over the best plane (S_2, S_3). This concludes the description of the blocks in Fig. 1(right). A remaining polarization ambiguity is finally removed by the rotation around the S_1 axis performed by the conventional V&V phase estimation block in Fig. 1(left).

It is worth noting that if two eigenvalues are very small, the fitting plane is not well identified. In this case, we force $\vec{v}_n$ to be orthogonal to the eigenvector with largest eigenvalue and to lie in the plane identified by such eigenvector and the previous stable result, i.e., $\vec{v}_{n-1}$.

Numerical Results

We first tested the algorithm on the toy XPolM model depicted in Fig. 3(top-right) to learn how to tune the algorithm parameters. In this model, a single-channel is added to ASE and the XPolM is emulated as a random time-varying rotation in Stokes space. By shaping as described in Fig. 3(top-left) the time autocorrelation function of the three angles $(\varphi, \varepsilon, \theta)$ that describe the unitary matrix $\mathbf{M}$, we controlled the desired amount of XPolM memory σ and strength δ. In a first set of simulations we fixed $\sigma = 30$ symbols and varied δ, to test the effectiveness of the fast compensator in presence of strong XPolM. Fig. 3(bottom-left) shows the Q-factor of the coherent receiver versus δ/π without and with the fast compensator with $L = 3$ taps. The compensator is able to reduce such strong lowpass fluctuations, with a Q-gain ranging from 0.5 to 2 dB.

In a second set of simulations we did the opposite, by fixing $\delta = \pi/2$ and varying the XPolM memory σ, see Fig. 3 (bottom-right). Here we also optimized the value of L at each point. In this case we note that the equalizer starts to gain after σ =15 symbols, when the lowpass behavior of XPolM can be tracked by the algorithm.

We then tested the algorithm in a realistic scenario by analyzing a 112 Gbit/s PDM-QPSK homogeneous WDM system propagated over 20×100 km dispersion managed link with pre compensation -650 ps/nm and 30 ps/nm residual dispersion per span (RDPS), see Fig. 1(left). The transmission fibers had a dispersion of 17 ps/nm/km, nonlinear index $\gamma = 1.3$ W^{-1}km^{-1} and zero PMD. The cumulated GVD was completely removed by an ideal lossless optical compensator before entering the receiver. The WDM comb was composed of 19 channels with 50 GHz spacing. Each channel was modulated by 1024 random symbols, and its carrier SOP randomly chosen over the Poincaré sphere. We loaded all the amplified

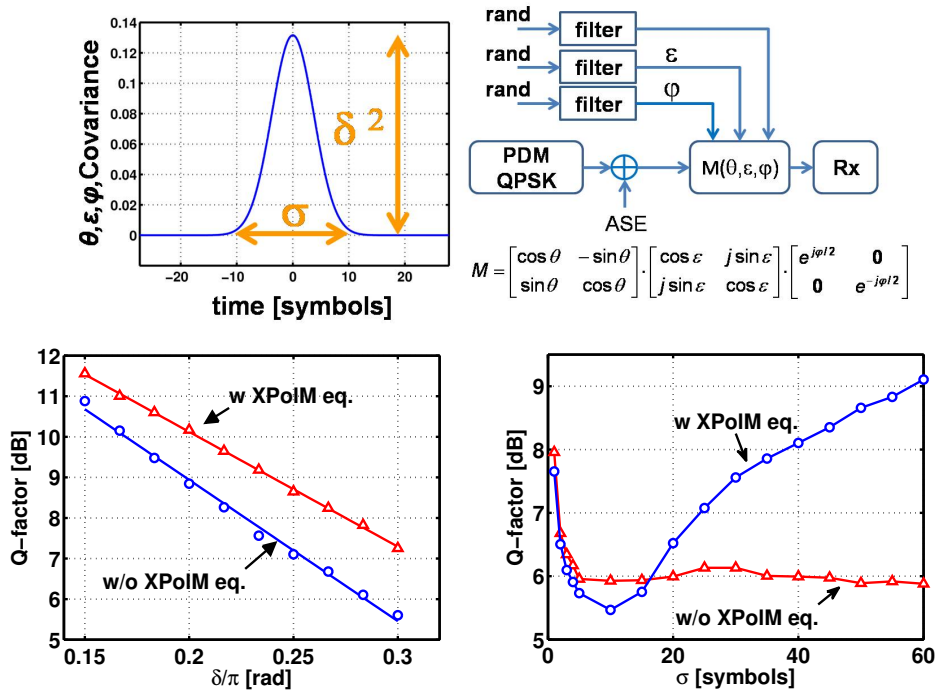

Fig. 3: Top-left: Toy XPolM model. Top-right: covariance function versus time (in symbols) of angles $(\varphi, \varepsilon, \theta)$. Bottom: XPolM model results showing Q-factor vs. XPolM strength δ (left), at fixed memory $\sigma = 30$ symbols and $L = 3$ taps, and Q-factor vs. XPolM memory σ (right) at $\delta = \pi/2$ with optimized L at each point.

spontaneous emission (ASE) noise at the end of the line with an equivalent noise figure per amplifier of 7 dB. We tested 10 random seeds, each corresponding to different WDM carrier SOPs and symbols, and for each seed we measured the bit error rate (BER) by counting at least 100 errors. Finally, we averaged the BER over the 10 seeds and then converted to Q-factor.

In the DSP we used a 7-tap CMA followed by a 27-tap V&V phase estimator. The fast XPolM compensator was implemented with a sliding window whose length was optimized at each power.

Fig. 4 shows the measured Q-factor. The gain in best Q-factor introduced by the fast XPolM compensator is about 1 dB and the optimal power is also increased by about 1 dB. It is worth noting that the best number of taps decreases for increasing powers because the contribution of the lowpass XPolM becomes dominant over ASE noise.

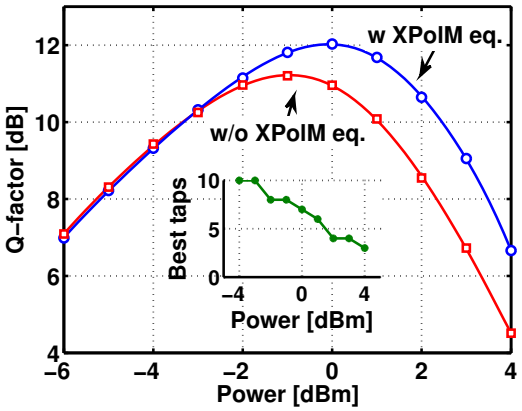

Fig. 4: 112 Gbit/s PDM-QPSK with and without the proposed algorithm. Inset: best number of taps.

Conclusions

We proposed a new blind feed-forward XPolM compensator for PDM-QPSK coherent transmissions, based on MMSE estimation in Stokes space. The equalizer is able to track the fast polarization scattering caused by interfering WDM symbols that quickly slide through the symbol of interest because of channel walk-off.

References

1 C. Xie, Photon. Technol. Letters, **21**, pp. 274–276 (2009).
2 D. Sperti et al., Photon. Technol. Letters, **23**, pp. 667-669 (2011).
3 E. F. Mateo et al., Optics Express, **19**, pp. 570–583 (2011).
4 L. Li et al., Proc. OFC'10 OWE3 (2010).
5 E. Ip et al., J. Lightw. Technol. **25**, pp. 2675–2692 (2007).